Sensor and Simulation Notes

Note 111

July 1970

Electromagnetic Interaction Between a Cylindrical Post and a Two-Parallel-Plate Simulator, I

by

R. W. Latham and K. S. H. Lee

Northrop Corporate Laboratories
Pasadena, California

Abstract

The time variation is obtained of the total current induced on a cylindrical post between a parallel-plate waveguide by a step-function plane wave traveling between the plates.

The resonant frequency and the decay time constant of the fundamental mode of the post current and the field enhancement factor, defined as the ratio of the maximum surface charge density to the late-time surface charge density on the end cap of the post, are calculated for various plate spacings and two given values of the post's diameter-to-length ratio. The frequency variation and the time history of the surface charge density on the end cap of the post are also given in graphical form for several values of plate separation.

Acknowledgment

We thank Mr. R. W. Sassman for his invaluable assistance in numerical computation, Dr. C. E. Baum for his many helpful suggestions, and Mrs. G. Peralta for her untiring aid in preparing the typescript and all the figures.

I. Introduction

This note is the continuation of a previous study on the electromagnetic interaction of a site structure with a two-parallel-plate simulator, with the site structure taller than the top plate of the simulator.[1] Here, we study the same problem for the case in which the top plate is higher than the site structure. The result of this study will be reported in two separate notes. The present note is devoted to calculating the response of a post to a step-function incident plane wave traveling between two parallel plates. In a subsequent note, a circular hole will be made in the top plate of the simulator and we will seek a "compromised" hole size for minimum electromagnetic interaction between the post and the simulator.

Recently, some results have been reported by Taylor and Steigerwald on the same problem that we are considering here.[2] However, there are several different aspects between their work and ours. Firstly, our approach to the problem differs from that of Taylor and Steigerwald. Our formulation is based on using the magnetic field and we arrive at an integral equation of the second kind for the axial current on the post, whereas their formulation is based on using the electric field and they end up with an integral equation of the first kind for the axial current with a constant determined by the boundary condition on the current at the "end" of the post. It is well known that an integral equation of the second kind is more suitable for numerical solution than one of the first kind.[3] Secondly, the effect of the end cap of the post is taken into account in this note. Thirdly, because we account for the effect of the end cap in a reasonably accurate way we can calculate the surface charge density there. The quantity of particular interest is the field enhancement factor defined as the ratio of the maximum surface charge density to the late-time surface charge density on the end cap when the post is exposed to a step-function incident wave.

In section II, an integral equation for the axial current on the post is derived by applying directly a Green's theorem for axisymmetric bodies. This integral equation is then solved numerically in section III. Numerical results are given in graphical form for the variation of the post current (a) with frequency at the base of the post, (b) along the post at resonant

frequencies, and (c) with the plate separation at resonant frequencies. We also calculate, for a step-function incident wave and for several plate separations, the time behavior of the post current from which we deduce its decay time constant for various plate separations. In section IV, we tabulate the field enhancement factor and give the frequency variation and time history of the surface charge density at the post's end for several plate spacings and two given values of the post's radius-to-length ratio.

II. Integral Equation for the Post Current

A direct application of equation (A.7) in reference 1 to the space between the parallel perfectly conducting plates and outside the perfectly conducting cylindrical post (Fig. 1) gives

$$H_\phi(\rho,z) = H_\phi^{inc}(\rho,z) + \int_0^h \left[H_\phi \frac{\partial}{\partial \rho'}(\rho' G)\right]_{\rho'=a} dz' + \int_0^a \left[H_\phi \frac{\partial}{\partial z'} G\right]_{z'=h} \rho' d\rho' \tag{1}$$

where G satisfies the equation

$$\left[\frac{\partial^2}{\partial \rho^2} + \frac{1}{\rho}\frac{\partial}{\partial \rho} - \frac{1}{\rho^2} + \frac{\partial^2}{\partial z^2} + k^2\right] G = -\delta(z - z')\frac{\delta(\rho-\rho')}{\rho'} \tag{2a}$$

between the two plates and the boundary conditions

$$\frac{\partial}{\partial z} G = 0 \quad \text{when} \quad z = 0, s \quad . \tag{2b}$$

For an incident harmonic plane wave given by

$$\underset{\sim}{H}^{inc} = -\underset{\sim}{e}_y H_o e^{ikx}$$

we have, after averaging with respect to ϕ,[1]

$$H_\phi^{inc} = -iH_o J_1(k\rho) \quad ,$$

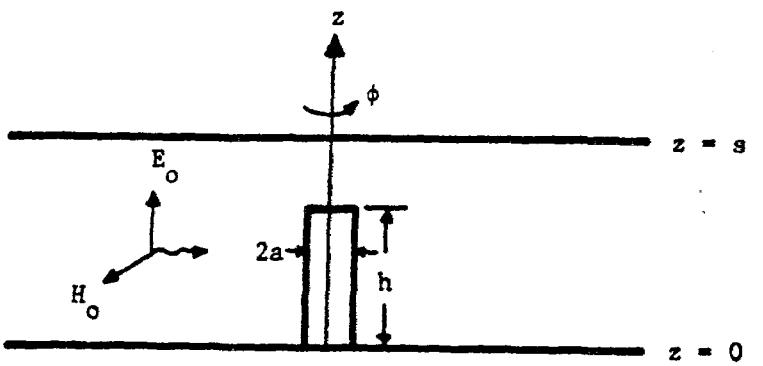

A

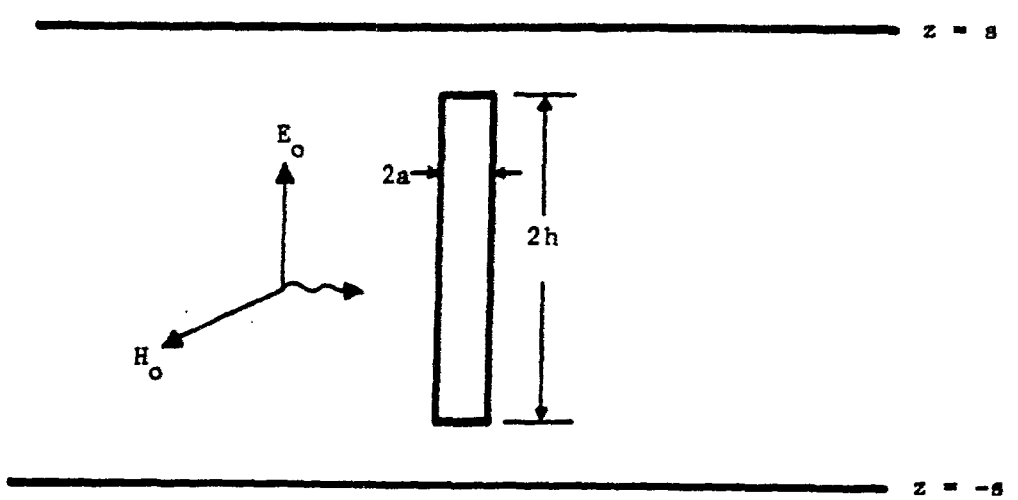

B

Figure 1. A cylindrical post between a parallel-plate waveguide: Two equivalent situations: A and B.

J_1 being the Bessel function of the first kind of order one. Defining

$$h_\phi(\rho,z) = H_\phi(\rho,z)/H_o$$

$$K(\rho,z;a,z') = -\left[\frac{\partial}{\partial\rho'}(\rho'G)\right]_{\rho'=a}$$

we obtain from (1)

$$\frac{1}{2}h_\phi(a,z) + \int_o^h K(a,z;a,z')h_\phi(a,z')dz'$$

$$= -iJ_1(ka) + \int_o^a \left[h_\phi \frac{\partial}{\partial z'}G\right]_{z'=h} \rho'd\rho' \qquad (3)$$

on the surface of the cylinder (i.e. $\rho = a$, $0 \le z \le h$). In terms of the currents $I(z) = 2\pi aH_\phi(a,z)$ and $I_e(\rho) = 2\pi\rho H_\phi(\rho,h)$, equation (3) becomes

$$\frac{1}{2}I(z) + \int_o^h K(a,z;a,z')I(z')dz'$$

$$= -2\pi iaH_oJ_1(ka) + a\int_o^a I_e(\rho')\left[\frac{\partial G}{\partial z'}\right]_{z'=h} d\rho' \qquad (4)$$

By assuming

$$I_e(\rho) = I(h)\left[1 - (1 - \rho^2/a^2)^{2/3}\right] \qquad (5)$$

one obtains an integral equation for I from (4). This assumption for I_e has been checked against the numerical solutions of the coupled integral equations involving I and I_e for $ka \leq 1.2$ in reference 3, and the accuracy of the assumption has been found to be excellent. It is expected that this assumption still holds true in the present situation if the separation between the top plate and the post's end is greater than the post's radius. In our subsequent numerical computation, equation (5) will be used.

We now proceed to find the Green's function G from (2). By the theory of images and equation (A.5) of reference 1 we can immediately write down

$$G(\rho,z;\rho',z') = \sum_{m=-\infty}^{\infty} \int_0^{2\pi} d\phi \cos\phi \left\{ \frac{e^{ikR_m^{(+)}}}{4\pi R_m^{(+)}} + \frac{e^{ikR_m^{(-)}}}{4\pi R_m^{(-)}} \right\} \tag{6}$$

where

$$R_m^{(+)} = \left[(2ms + z + z')^2 + \rho^2 + \rho'^2 - 2\rho\rho' \cos\phi\right]^{\frac{1}{2}}$$

$$R_m^{(-)} = \left[(2ms - z + z')^2 + \rho^2 + \rho'^2 - 2\rho\rho' \cos\phi\right]^{\frac{1}{2}} .$$

Equations (4), (5) and (6) constitute the mathematical formulation of our problem.

III. Numerical Results

The integral equation (4) for the post current was numerically solved with the aid of an electronic computer for two values of a/h (.1 and .01) and several values of h/s. Figures 2a and 2b are plots of the post current at the base (z = 0) against kh. It is seen from these plots that the resonant frequencies are quite insensitive to the separation of the two plates. For a/h = .1, $k_o h \approx 1.3$ and for a/h = .01, $k_o h \approx 1.5$, where k_o is the wave number of the first resonance of the post current. These values of k_o apply to all plate separations within 10% or so. Figures 3a and 3b show the variation of the current at k_o along the post. In Fig. 4 the magnitude of the post current at k_o normalized with respect to that for infinite plate separation is plotted against the plate separation. For s/h > 3 the two curves in Fig. 4 oscillate about unity with decreasing amplitude. This phenomenon is expected from the interactions of the post with its images.

For a step-function incident plane wave whose magnetic field vector is

$$\underset{\sim}{H}^{inc}(x,t) = - \underset{\sim}{e}_y H_o U(t - x/c)$$

the time history of the post current at z = 0 is plotted in Figs. 5a and 5b for a/h = .1 and in Figs. 6a and 6b for a/h = .01 with the plate separation as a parameter.

The decay time, τ_s, of the fundamental mode of the post current normalized with respect to the free-space value τ_∞ (i.e., when the two plates are separated infinitely far apart) is given in Table I and also plotted in Fig. 7. Note that in Table I we tabulate τ_s/τ_∞ for various values of h/s, while in Fig. 7 we plot τ_s/τ_∞ against s/h. The values of τ_s were obtained by fitting the envolopes of the curves in Figs. 5b and 6b to an exponential curve $\exp[- ct/(h\tau_s)]$.

One can see from Figs. 5a and 5b that the quantity, $I(0,t)/(hH_o)$, reaches its maximum value 2.52 at ct/h = 1.1 for a/h = .1, and that it reaches its maximum value 1.34 at ct/h = 1.0 for a/h = .01. These maximum values hold true for all plate separations within 2% or so.

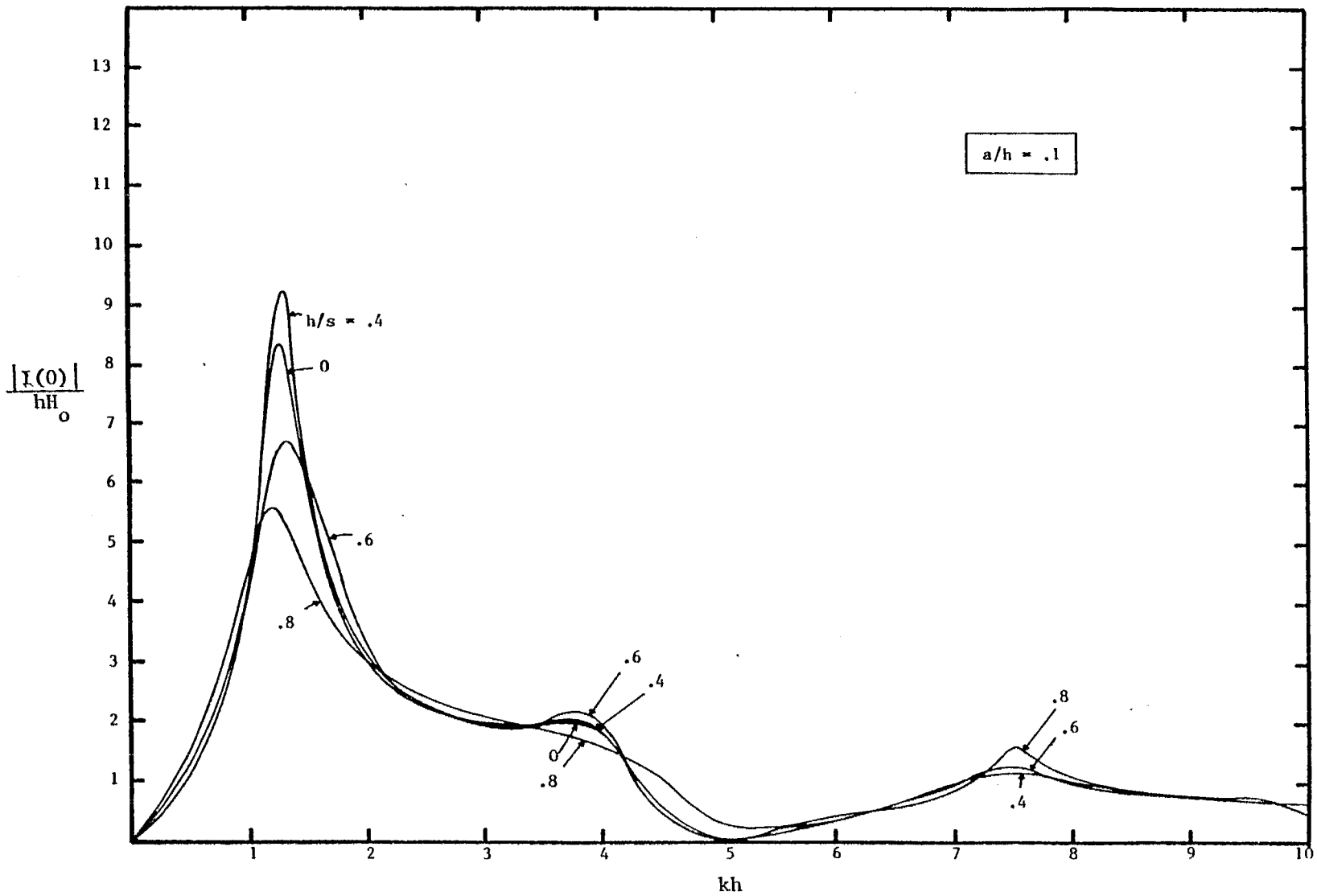

Figure 2a. Post current at z = 0 versus frequency.

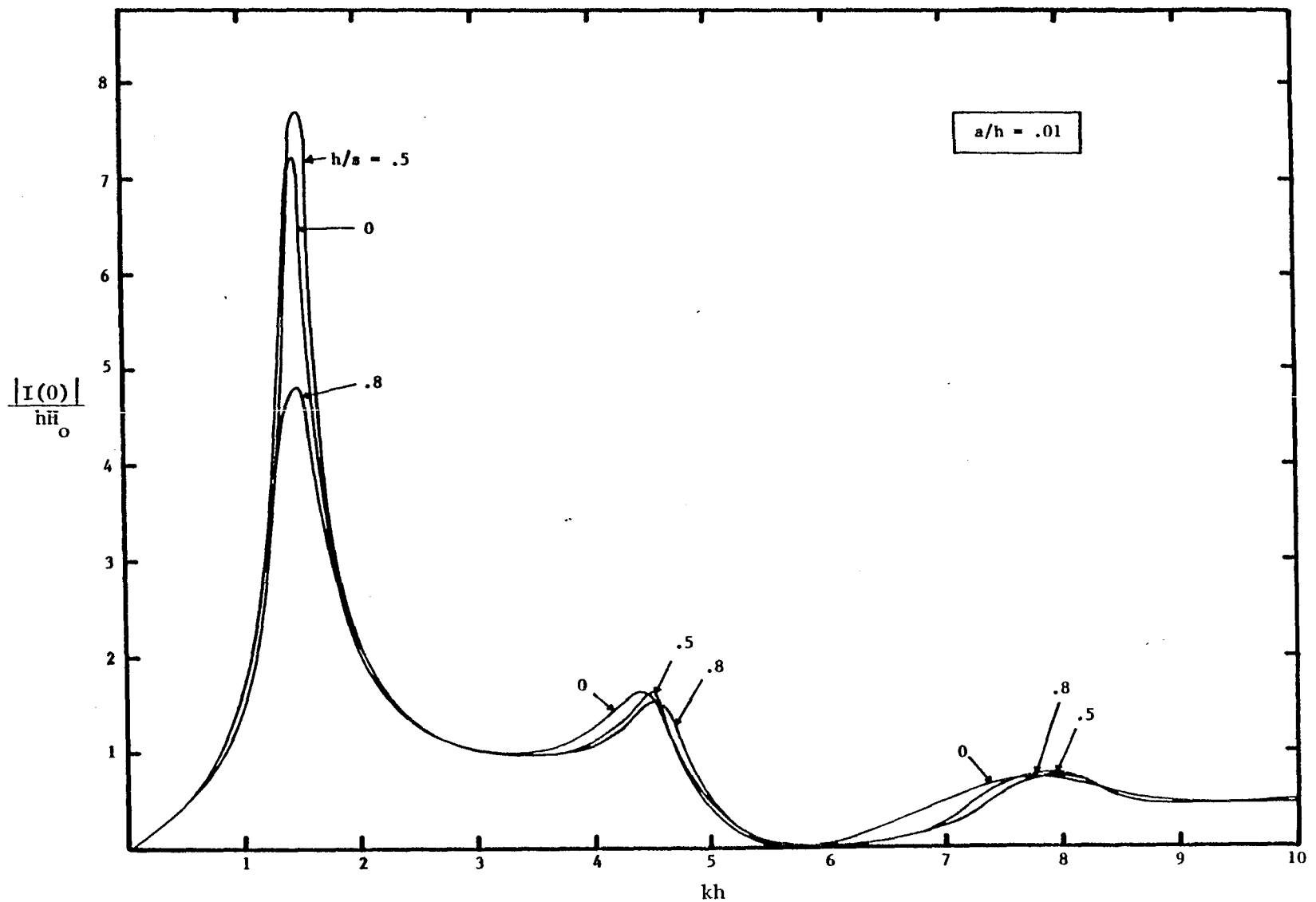

Figure 2b. Post current at z = 0 versus frequency.

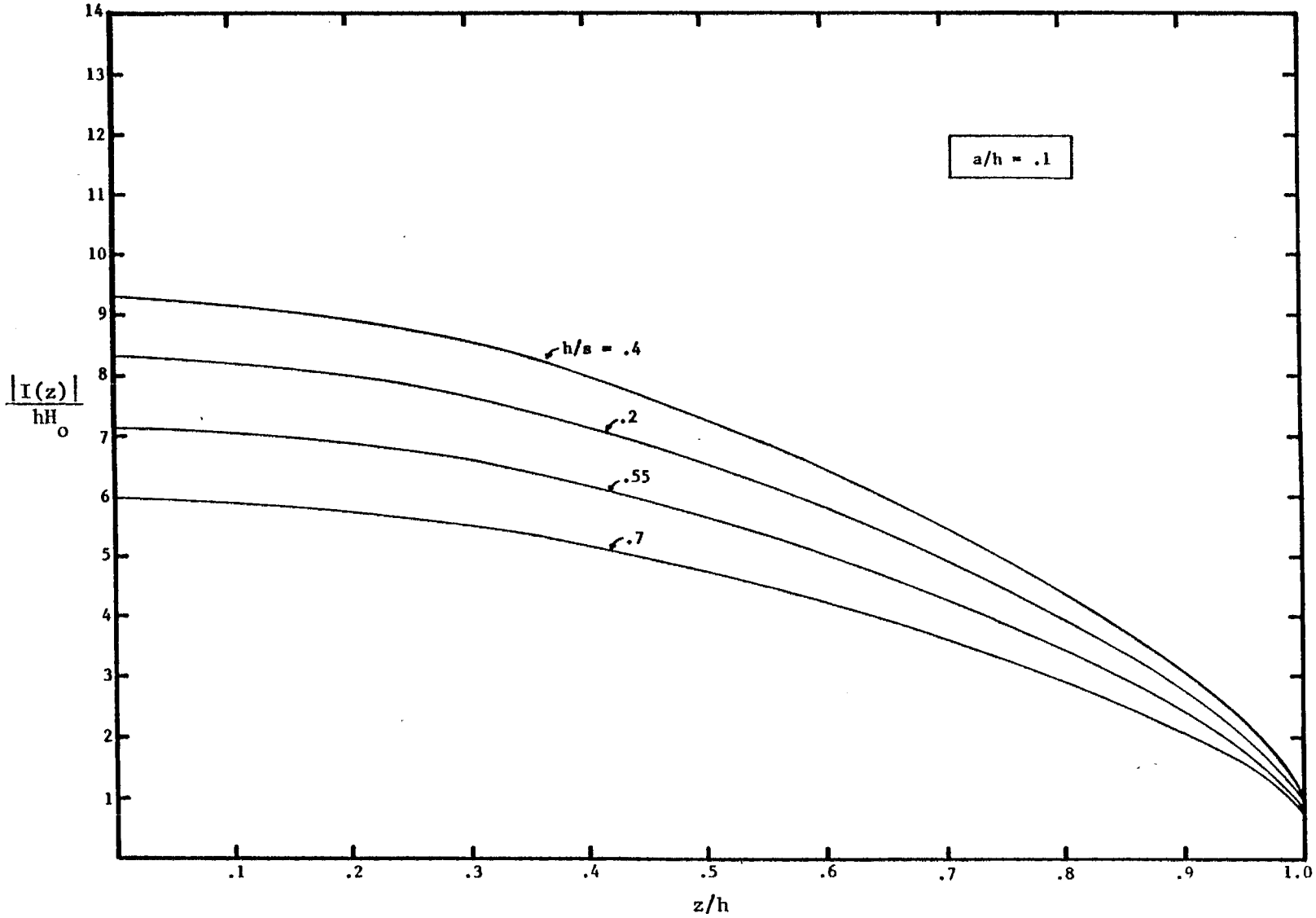

Figure 3a. Magnitude of current versus position around resonant frequency ($k_o h = 1.3$).

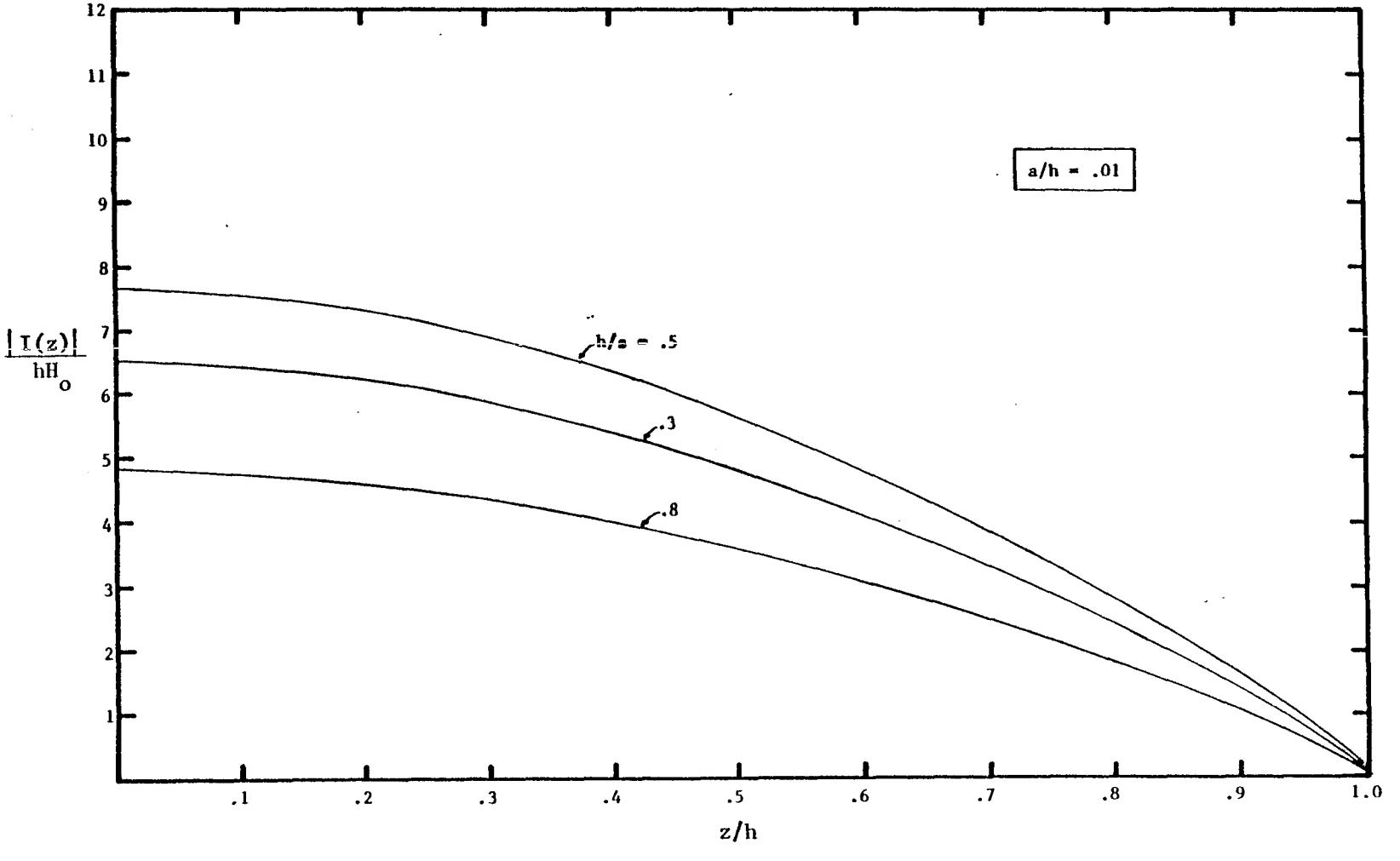

Figure 3b.[4] Magnitude of current versus position around resonant frequency ($k_o h = 1.5$).

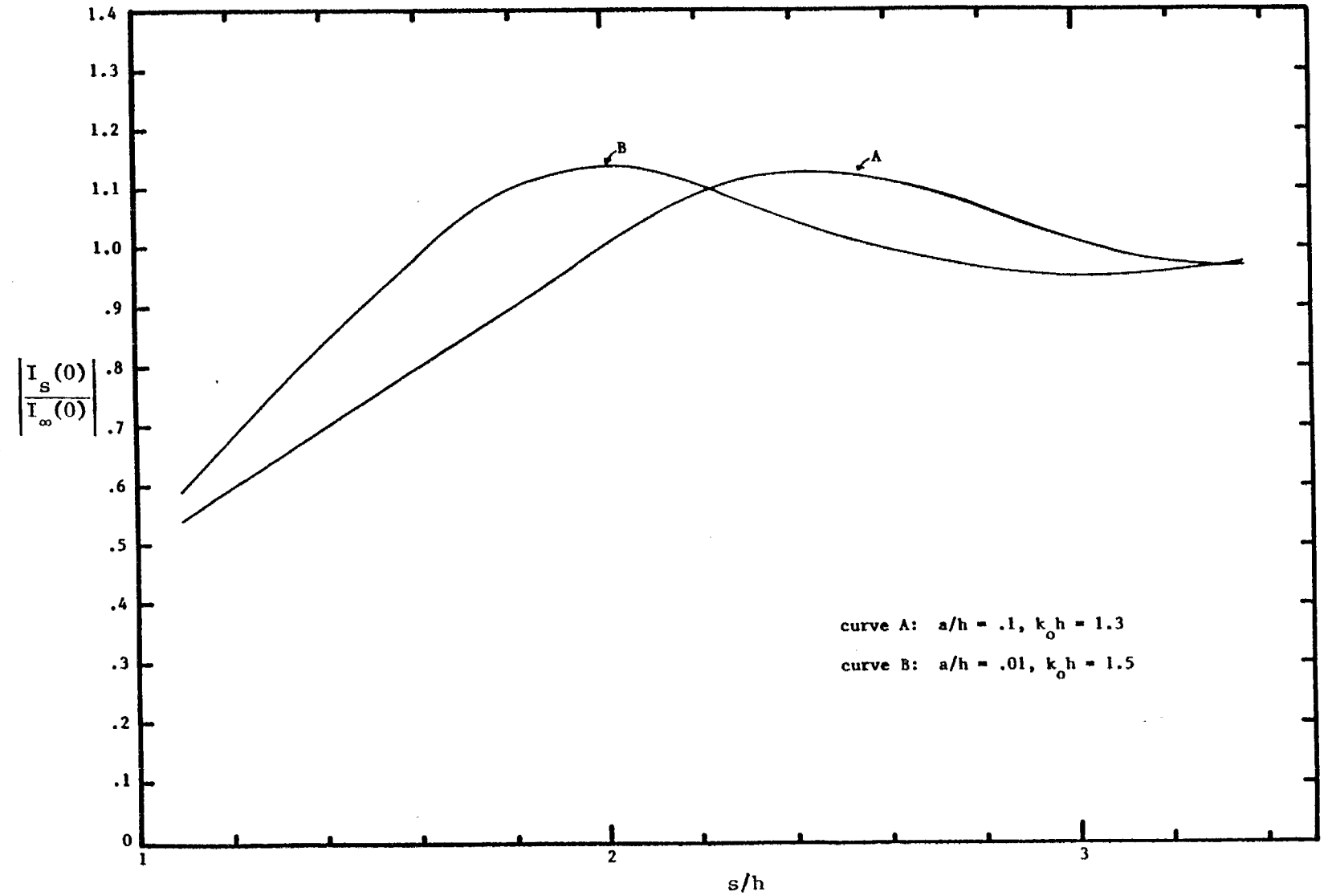

Figure 4. Post current at z = 0 versus plate separation around the resonant frequency.

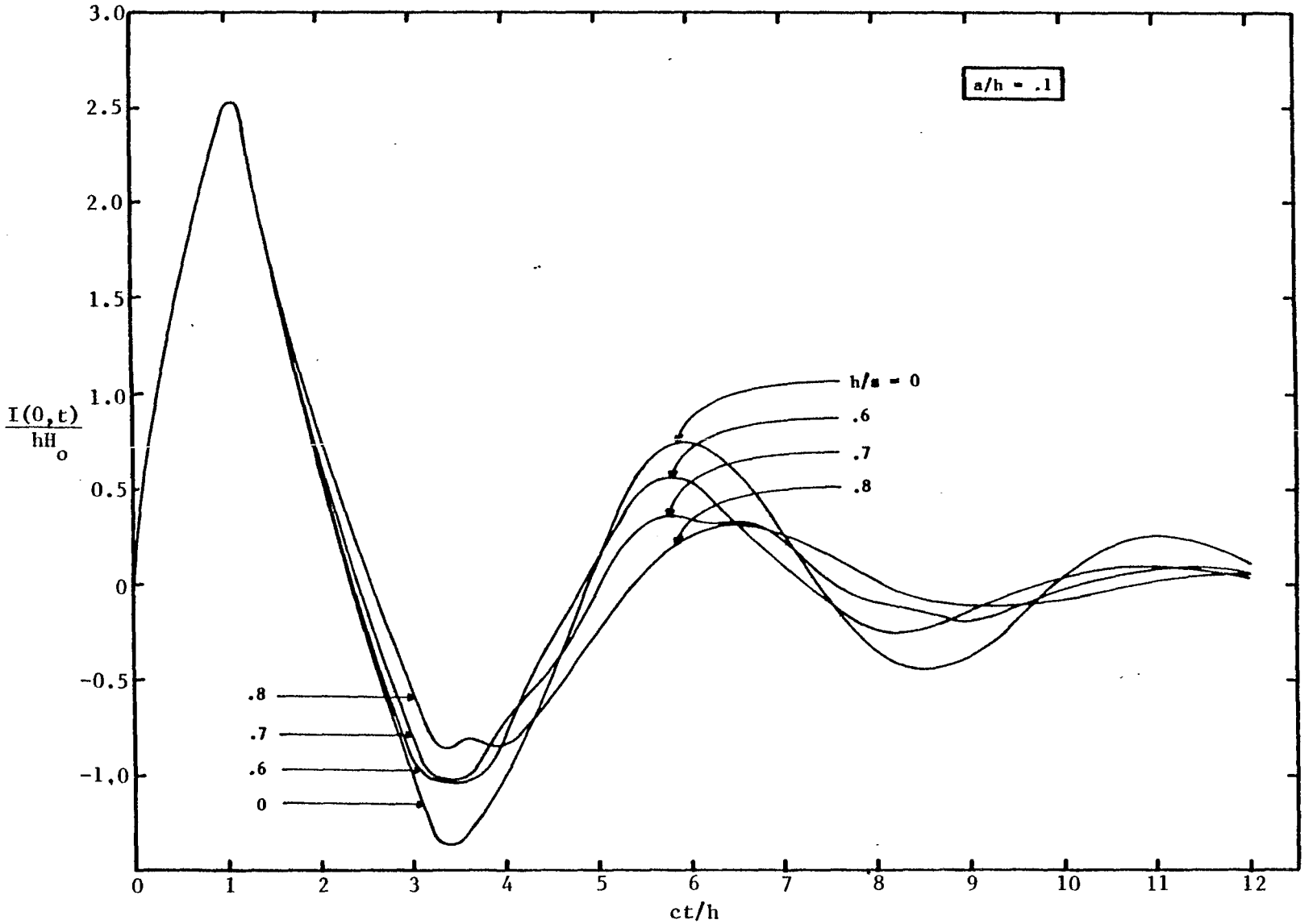

Figure 5a. Time history of post current at z = 0 with plate separation as parameter.

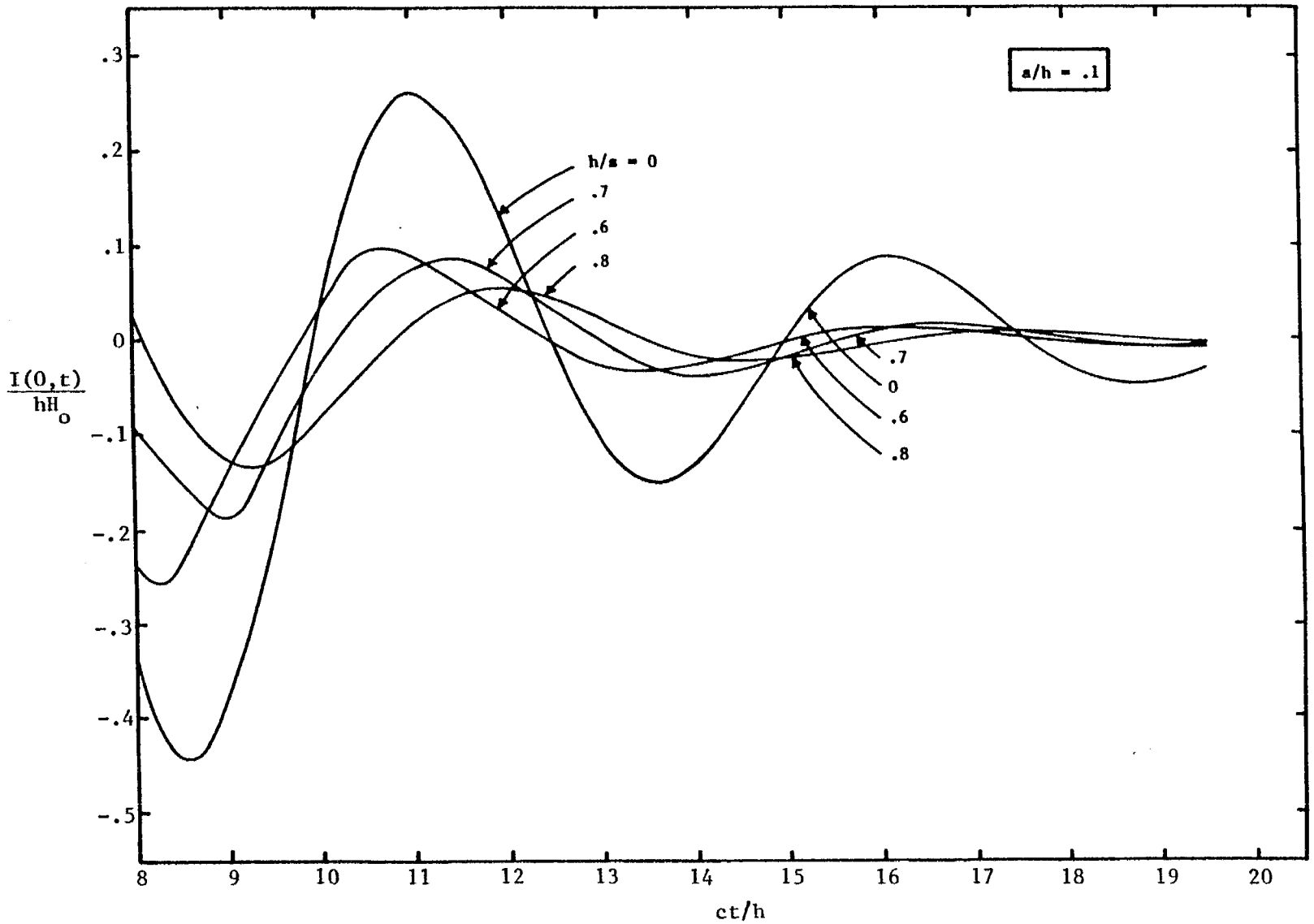

Figure 5b. Time history of post current at z = 0 with plate separation as parameter.

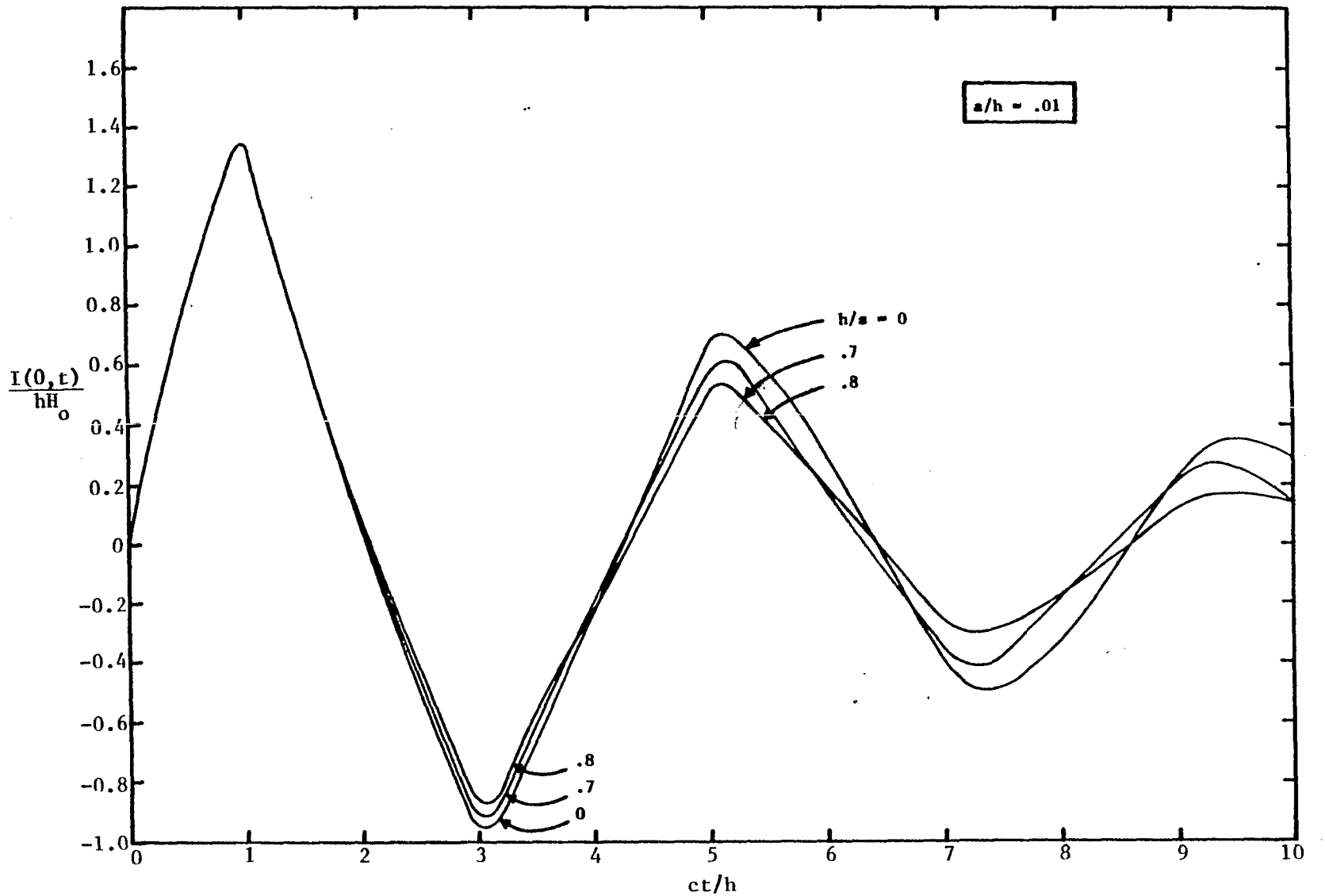

Figure 6a. Time history of post current at z = 0 with plate separation as parameter.

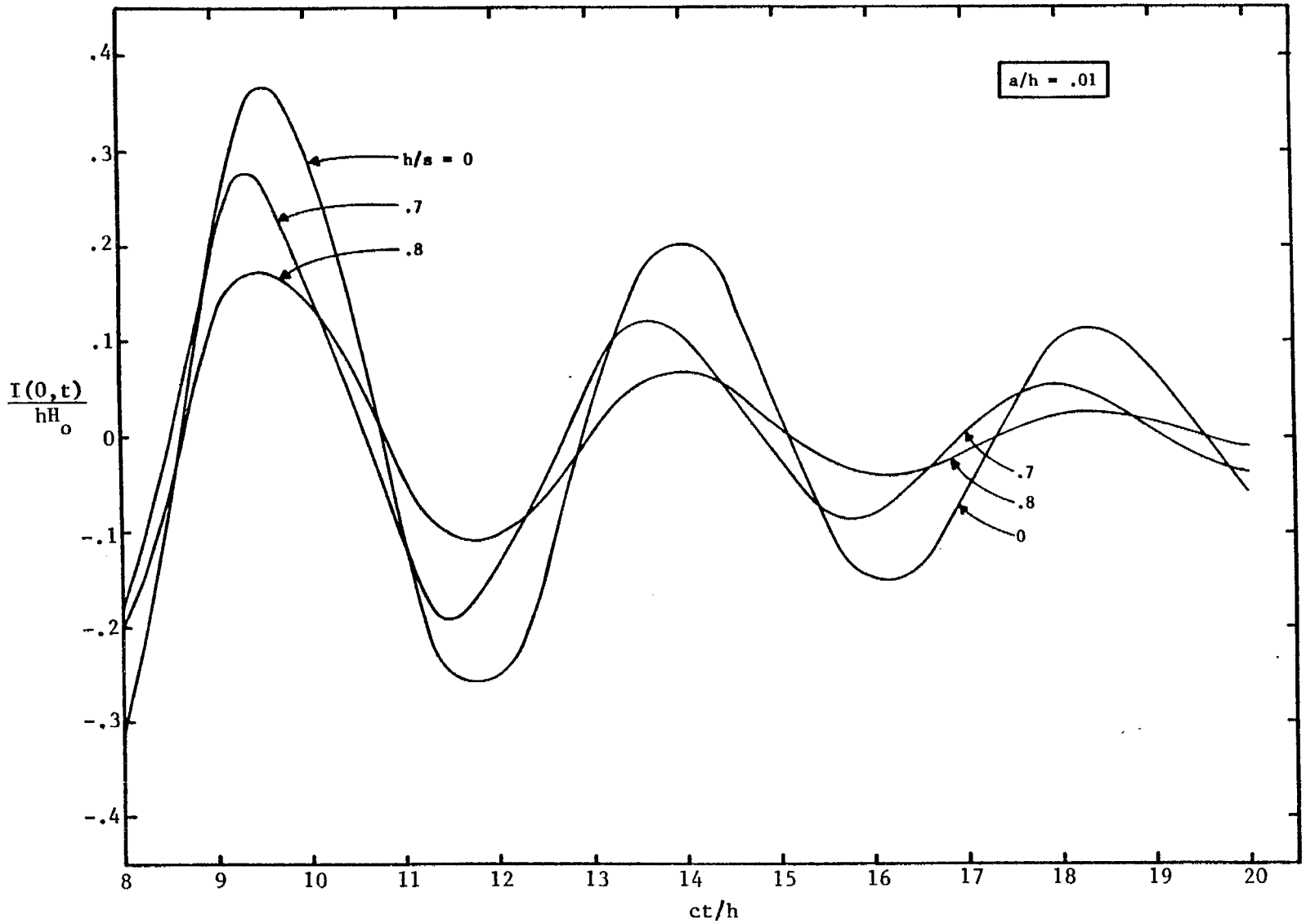

Figure 6b. Time history of post current at z = 0 with plate separation as parameter.

Table I. Decay time

(τ_∞ = 4.732 for a/h = .1, τ_∞ = 7.325 for a/h = .01)

h/s	τ_s/τ_∞ (a/h = .1)	τ_s/τ_∞ (a/h = .01)
.9	.646	.541
.8	.650	.611
.7	.625	.760
.6	.579	.965
.5	.938	1.170
.4	1.231	1.140
.3	1.074	.903
0	1.000	1.000

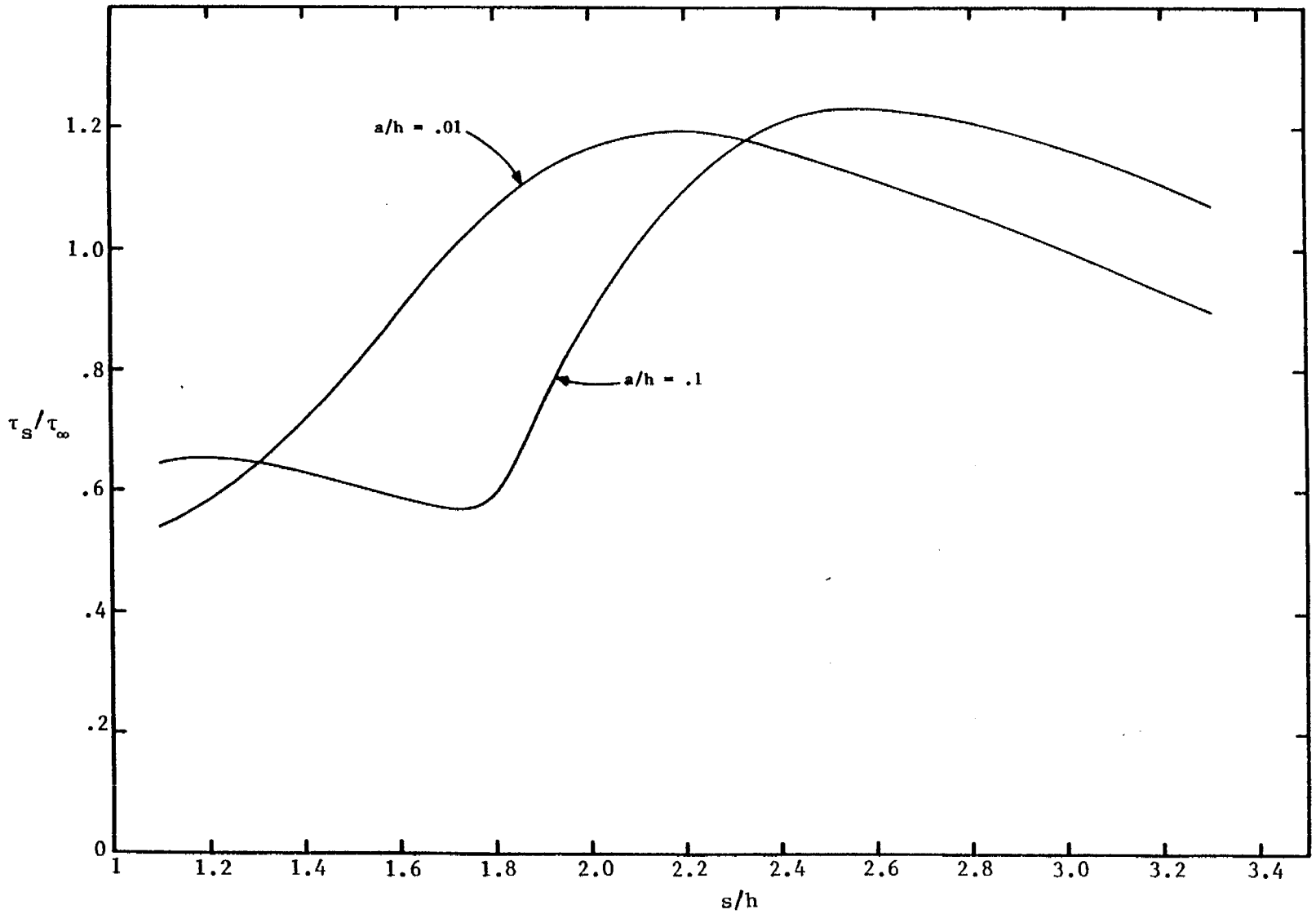

Figure 7. Decay time versus plate separation (as s/h increases, the curves oscillate about unity with decreasing amplitudes).

IV. Field Enhancement at the Post's End

Referring to the two-parallel-plate EMP simulator depicted in Fig. 1 one would naturally worry about the air breakdown near the end of the post where the electric field strength is most intense. To estimate the field strength there we will calculate the surface charge density, σ_o, from a knowledge of the total axial current at the post's end (i.e., $z = h$), since the surface charge density is a measure of the total electric field on a perfect conductor. σ_o thus calculated is then the surface charge density averaged with respect to ϕ, which is the same thing as the zeroth mode in the Fourier series expansion of $\sigma = \sum_{m=o}^{\infty} \sigma_m \cos m\phi$.

Integrating the continuity equation

$$\nabla \cdot \underset{\sim}{K} = - \frac{\partial \sigma}{\partial t} \tag{7}$$

over a disk on the end of the post (i.e., a disk defined by $z = h$, $0 < \rho < a$), one immediately gets

$$\frac{d}{d\rho} I_e(\rho,t) = 2\pi\rho \frac{\partial \sigma_o}{\partial t} \tag{8}$$

where

$$- I_e(\rho,t) = \int_o^{2\pi} K_\rho(\rho,\phi,t)\rho d\phi$$

$$\sigma_o(\rho,t) = \frac{1}{2\pi} \int_o^{2\pi} \sigma(\rho,\phi,t) d\phi$$

We now substitute (5) into (8) to get

$$\frac{\partial \sigma_o}{\partial t} = \frac{2}{3\pi a^2} I(h,t) \cdot (1 - \rho^2/a^2)^{-1/3} \tag{9}$$

which, upon integration and after normalization, gives

$$\frac{\sigma_o(\rho,t)}{\varepsilon_o E_o} = \frac{2}{3\pi}\left(\frac{h}{a}\right)^2 \int_o^{ct/h} \frac{I(h,t')}{hH_o}\, d\left(\frac{ct'}{h}\right) \cdot (1 - \rho^2/a^2)^{-1/3} \qquad (10)$$

In the frequency domain (9) becomes, after normalization,

$$\frac{\sigma_o}{\varepsilon_o E_o} = \frac{2i}{3\pi}\left(\frac{h}{a}\right)^2 \frac{1}{kh}\left[\frac{I(k,h)}{hH_o}\right] \cdot (1 - \rho^2/a^2)^{-1/3} \qquad (11)$$

Note that (11) has the appropriate singular behavior at low frequencies. We have checked equation (11) against some accurate numerical calculations[5] for the case a/h = .25 and kh = 0, and only 3% difference was found in the two different methods of calculation. The agreement would become better as a/h gets smaller.

In Table II, we give the values of C_s, C_r/C_s and C_m/C_s for various values of h/s, where

$$C_s = \frac{2}{3\pi}\left(\frac{h}{a}\right)^2 \lim_{kh\to 0} \frac{|I(k,h)|}{(kh)(hH_o)}$$

$$C_r = \frac{2}{3\pi}\left(\frac{h}{a}\right)^2 \frac{|I(k,h)|}{(kh)(hH_o)} \qquad \text{for} \begin{cases} kh = 1.3 \text{ when } a/h = .1 \\ kh = 1.5 \text{ when } a/h = .01 \end{cases}$$

$$C_m = \frac{2}{3\pi}\left(\frac{h}{a}\right)^2 \int_o^{\tau_1} \frac{I(h,t)}{hH_o}\, d\left(\frac{ct}{h}\right), \quad \tau_1 = \text{the first zero crossing in the time-history curves of the current}$$

If one wishes, one can call C_r/C_s the field enhancement factor at the first resonant frequency and C_m/C_s the maximum field enhancement factor.

Figures 8a and 8b display the frequency variation of the surface charge density with the plate spacing as a parameter. It can be seen that the resonant frequencies are quite insensitive to the plate separation. In these figures, C_k is defined to be the coefficient of equation (11), i.e.,

$$C_k = \frac{2}{3\pi}\left(\frac{h}{a}\right)^2 \frac{|I(k,h)|}{(kh)(hH_o)} .$$

Table II. Surface charge density on the post's end

	a/h = .1			a/h = .01		
h/s	C_s	C_r/C_s	C_m/C_s	C_s	C_r/C_s	C_m/C_s
.9	17.013	1.086	1.448	77.88	2.434	1.667
.8	11.805	1.502	1.465	71.19	2.993	1.667
.7	10.651	1.744	1.483	69.20	3.596	1.684
.6	10.171	1.990	1.501	68.27	4.335	1.691
.5	9.940	2.422	1.513	67.76	4.771	1.701
.4	9.810	2.762	1.532	67.50	4.301	1.709
.3	9.751	2.416	1.541	67.35	4.098	1.713
0	9.715	2.502	1.547	67.27	4.244	1.715

The time history of the surface charge density is plotted in Figs. 9a and 9b. As time increases, these curves oscillate about unity with decreasing amplitudes. In these figures, C_t is defined as the coefficient of equation (10), i.e.,

$$C_t = \frac{2}{3\pi} \left(\frac{h}{a}\right)^2 \int_0^{ct/h} \frac{I(h,t')}{hH_o} \, d\left(\frac{ct'}{h}\right) \quad .$$

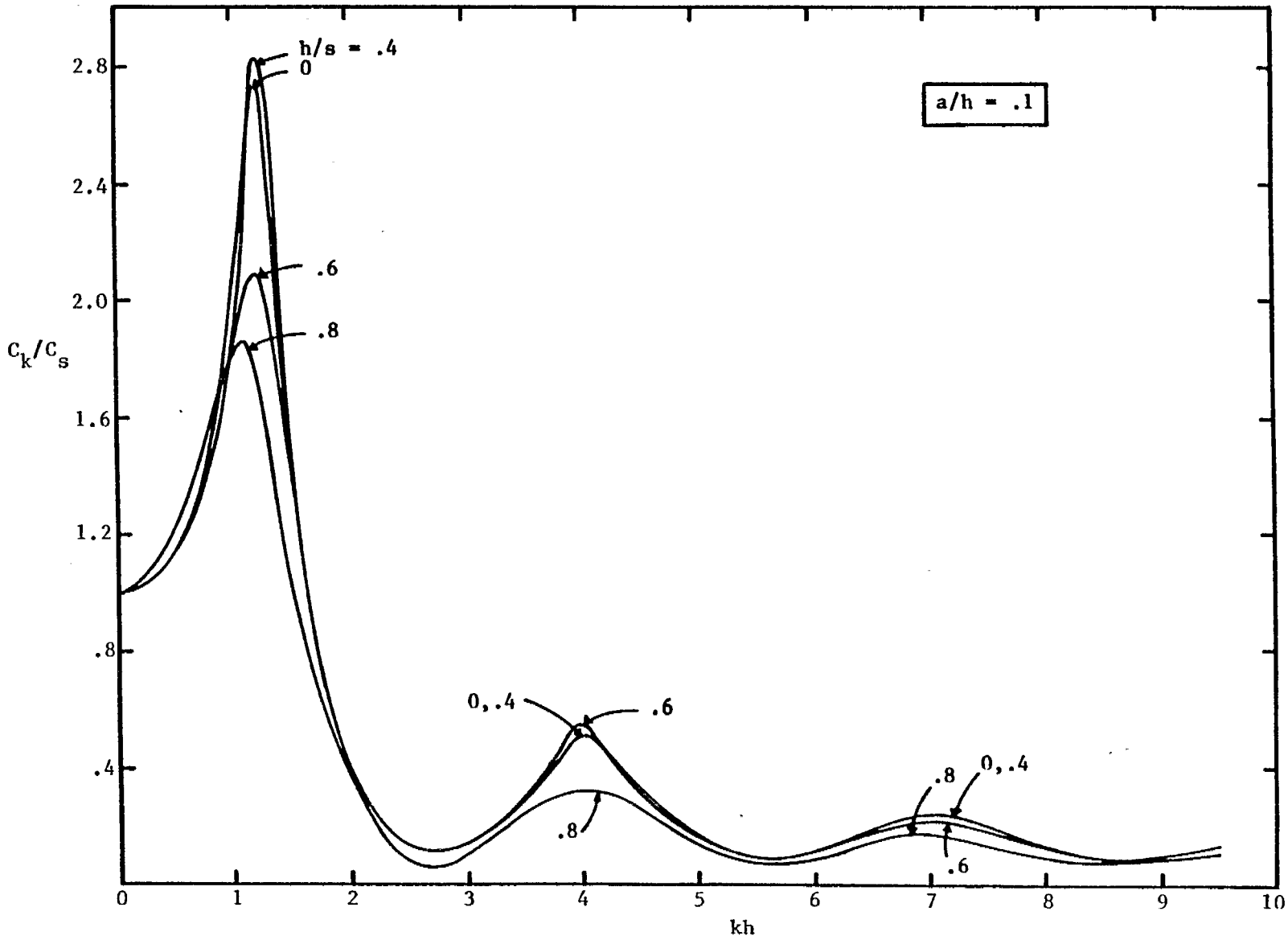

Figure 8a. Frequency variation of surface charge density at the post's end with plate separation as parameter.

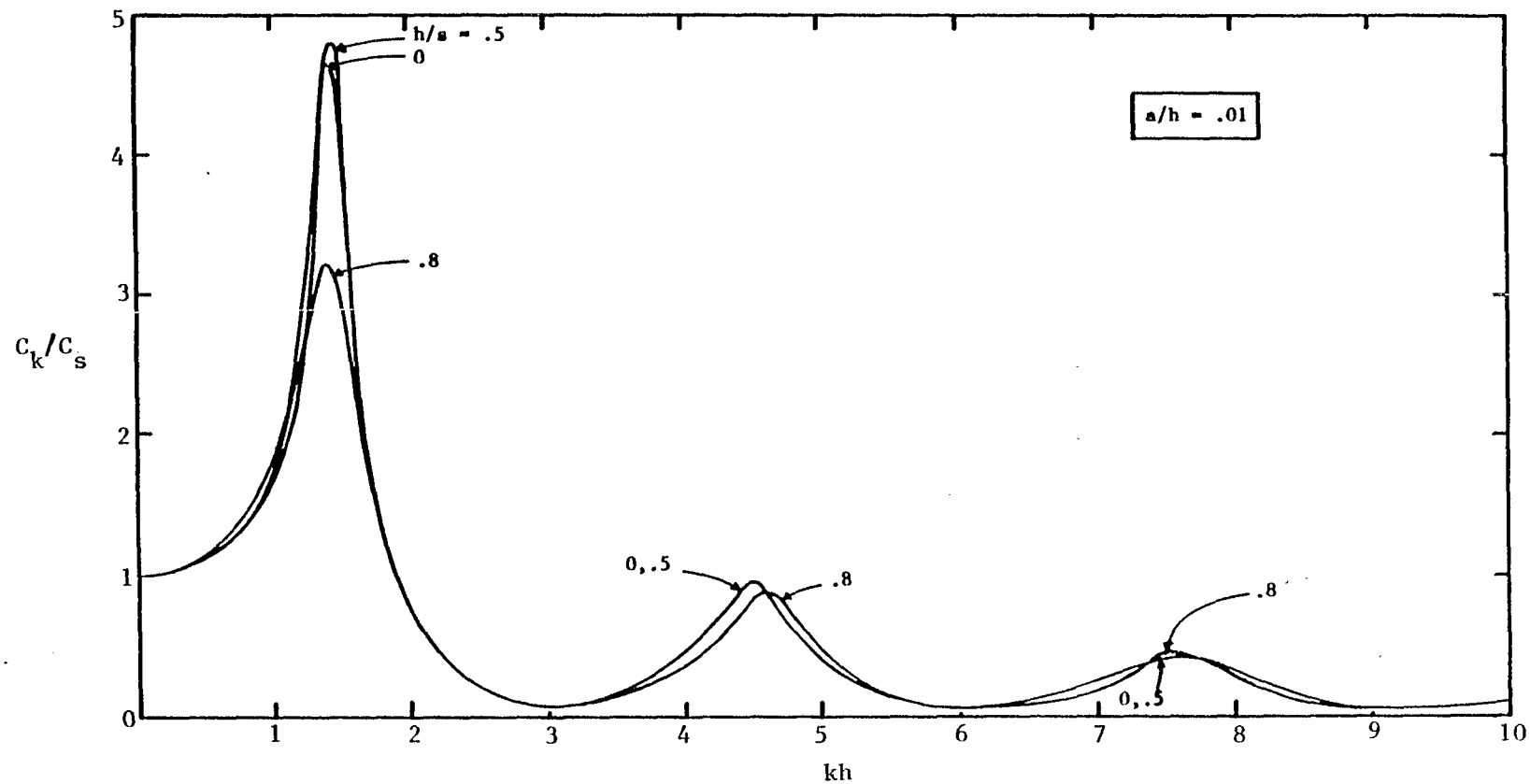

Figure 8b. Frequency variation of surface charge density at the post's end with plate separation as parameter.

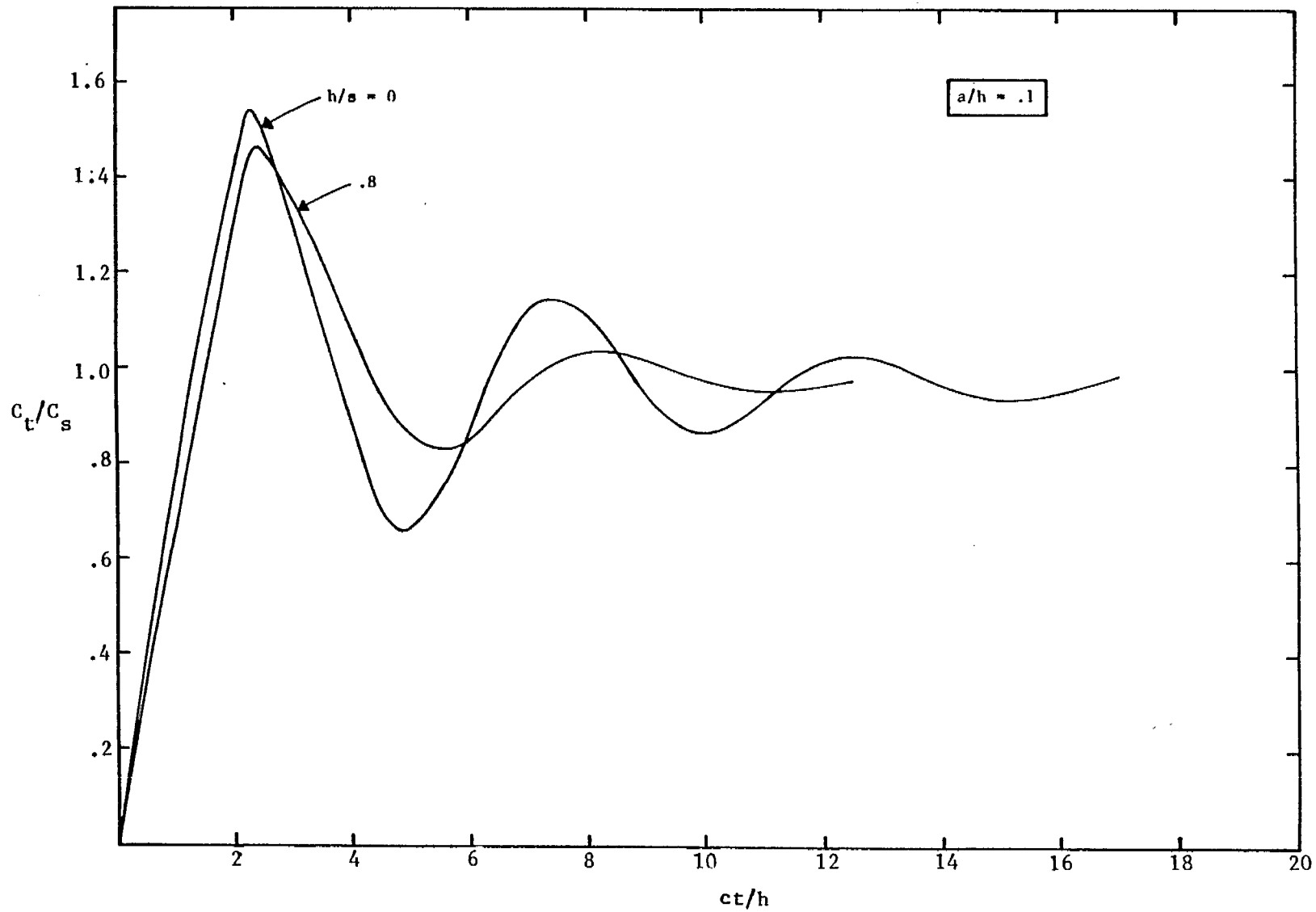

Figure 9a. Time history of surface charge density at the post's end with plate separation as parameter.

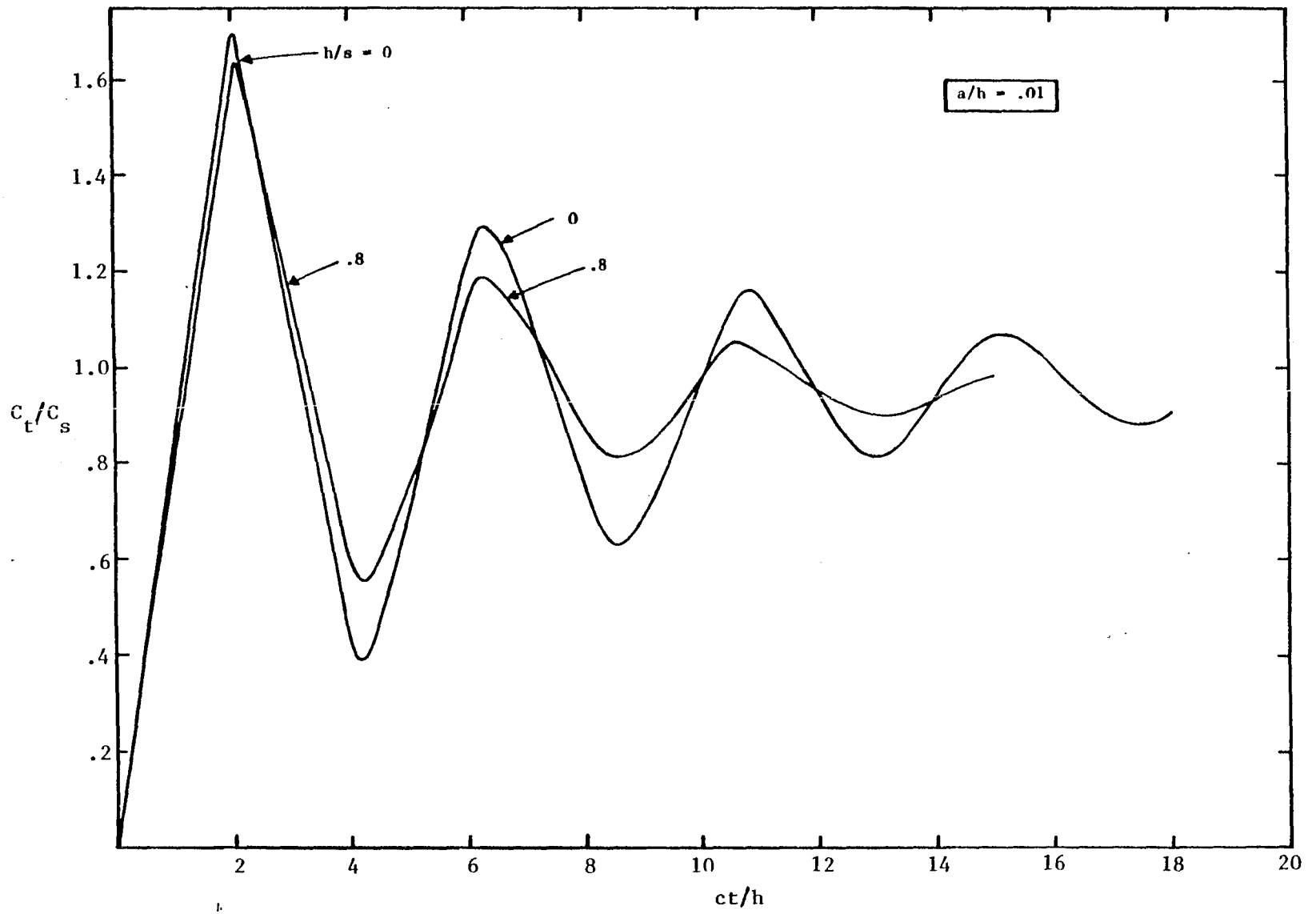

Figure 9b. Time history of surface charge density at the post's end with plate separation as parameter.

References

1. R. W. Latham, K. S. H. Lee, and R. W. Sassman, "Minimization of current distortion on a cylindrical post piercing a parallel-plate waveguide," Sensor and Simulation Notes, No. 93, September 1969.
2. C. D. Taylor and G. A. Steigerwald, "On the pulse excitation of a cylinder in a parallel plate waveguide," Sensor and Simulation Notes, No. 99, March 1970.
3. D. L. Phillips, "A technique for the numerical solution of certain integral equations of the first kind," J. Assoc. Comput. Machinery, 9, pp. 84-97, 1962.
4. R. W. Sassman, "The current induced on a finite, perfectly conducting, solid cylinder in free space by an electromagnetic pulse," EMP Interaction Note XI, July 1967.
5. T. T. Taylor, "Electric polarizability of a short right circular conducting cylinder," J. Res. NBS, 64B, No. 3, p. 135, 1960.

SSN 111

Errata Sheet No. 1

R. W. Latham and K. S. H. Lee, "Electromagnetic Interaction Between a Cylindrical Post and a Two-Parallel-Plate Simulator, I" SSN 111, July 1970.

On page 23, Table II should read as follows:

	a/h = .1			a/h = .01		
h/s	C_s	C_r/C_s	C_m/C_s	C_s	C_r/C_s	C_m/C_s
.9	10.680	1.086	1.448	37.50	2.434	1.667
.8	7.512	1.502	1.465	34.36	2.993	1.667
.7	6.784	1.744	1.483	33.40	3.596	1.684
.6	6.481	1.990	1.501	32.96	4.335	1.691
.5	6.332	2.422	1.513	32.72	4.771	1.701
.4	6.250	2.762	1.532	32.57	4.301	1.709
.3	6.213	2.416	1.541	32.51	4.098	1.713
0	6.120	2.502	1.547	32.38	4.244	1.715

SSN 111

Errata Sheet No. 1

R. W. Latham and K. S. H. Lee, "Electromagnetic Interaction Between a Cylindrical Post and a Two-Parallel-Plate Simulator, I" SSN 111, July 1970.

On page 23, Table II should read as follows:

	a/h = .1			a/h = .01		
h/s	C_s	C_r/C_s	C_m/C_s	C_s	C_r/C_s	C_m/C_s
.9	10.680	1.086	1.448	37.50	2.434	1.667
.8	7.512	1.502	1.465	34.36	2.993	1.667
.7	6.784	1.744	1.483	33.40	3.596	1.684
.6	6.481	1.990	1.501	32.96	4.335	1.691
.5	6.332	2.422	1.513	32.72	4.771	1.701
.4	6.250	2.762	1.532	32.57	4.301	1.709
.3	6.213	2.416	1.541	32.51	4.098	1.713
0	6.120	2.502	1.547	32.38	4.244	1.715